Electrochimica Acta 210 (2016) 520–529

Contents lists available at ScienceDirect

Electrochimica Acta

journal homepage: www.elsevier.com/locate/electacta

Surface Limited Redox Replacement Deposition of Platinum Ultrathin Films on Gold: Thickness and Structure Dependent Activity towards the Carbon Monoxide and Formic Acid Oxidation reactions

Zakiya Al Amri[a], Michael P. Mercer[a,b,1], Natasa Vasiljevic[a,b,2,*]

[a] School of Physics, H.H. Wills Physics Laboratory, University of Bristol, Bristol, BS8 1TL, UK
[b] Bristol Centre for Functional Nanomaterials, University of Bristol, Bristol, BS8 1FD, UK

ARTICLE INFO

Article history:
Received 1 February 2016
Received in revised form 22 May 2016
Accepted 23 May 2016
Available online 24 May 2016

Keywords:
Surface Limited Redox Replacement
Pt-Au
Pt-bimetallic nanostructures
CO stripping
Formic Acid Oxidation

ABSTRACT

The Surface Limited Redox Replacement (SLRR) method in one-cell configuration has been used to grow Pt ultra-thin films on Au using two different sacrificial underpotentially deposited (UPD) layers: Cu and Pb. The Pt films grown by multiple Pb UPD-SLRR cycles (1–10) exhibit comparable roughness as determined by integration of the H UPD charge. In contrast to that, due to the 2:1 stoichiometry of the replacement between Cu UPD layer and $PtCl_4^{2+}$ ions, the Pt films grown by Cu UPD-SLRR show a steady increase of the roughness with the number of deposition cycles (1–10). The differences in the structure of the films have been used as a platform to study the stripping of pre-adsorbed CO and the formic acid oxidation (FAO) reaction as a function of their thickness. On Pt films of comparable roughness grown by SLRR of Pb UPD, the CO stripping peak shows no significant changes in the onset potential and a small peak maximum shift of ~7 mV between the film of lowest (1 ML) and all higher thicknesses (2–10 ML). However, Pt films grown by SLRR of Cu UPD show a larger potential window of differences of ~26 mV over which the peak maximum potentials shift more negative with the number of deposition cycles. The most positive CO stripping potential obtained for a sub-ML Pt (~0.56 ML) grown by a single SLRR cycle suggests CO is more strongly bonded than on films grown by multiple replacements that completely cover the Au substrate. The measured activity toward FAO is in agreement with the CO electro-oxidation results. No significant differences in the activity for FAO have been observed on Pt films of comparable roughness grown by SLRR of Pb UPD which show activity close to that of pure Pt. However, a more significant change of FAO reactivity has been measured for Pt films grown via SLRR of Cu UPD with the highest activity measured for a sub-ML Pt deposit. Following subsequent replacements, the FAO activity tends towards that of pure Pt. The observed differences in the catalytic behaviour of Pt films grown by SLRR are the result of the differences in their morphology and the nanocluster structure of the films. On sub-monolayer Pt films, the behaviour is dominated by nanocluster size and coverage of the deposit. For a completely covered surface of Au, the effect of roughness of Pt films and nanocluster nature of the deposit has a dominant role in the behaviour and activity.

1. Introduction

A demand for low-cost, highly active and stable Pt catalysts for fuel cell applications has been driving the development of new Pt nanostructures in which atomic scale effects and phenomena can be exploited [1–4]. Pt-bimetallic nanostructures in particular, such as strained overlayers, Pt-X alloys or ordered intermetallics, and `Pt-nanoclusters (2D and 3D) have been actively pursued on different types of metal systems. The reduced dimensionality (from 3D to 2D and 1D) in combination with the bonding to another metal, generally results in electronic, and geometrical effects that can substantially alter the catalytic activity and selectivity [4–6].

In the case of Pt bimetallic nanostructures, there are many structural variables such as the crystallographic orientation i.e. shape, size, morphology, and surface composition that play a role in the catalytic behaviour and activity. A complete fundamental

* Corresponding author at: School of Physics, H.H. Wills Physics Laboratory, University of Bristol, Bristol, BS8 1TL, UK. Tel.: +44 0 117331739.
E-mail address: n.vasiljevic@bristol.ac.uk (N. Vasiljevic).
[1] Current address: Department of Chemistry, Lancaster University, Lancaster, LA1 4YB, United States.
[2] ISE Member.

http://dx.doi.org/10.1016/j.electacta.2016.05.161

understanding of the role of these effects is difficult to decouple and, therefore, studies on simple and well-defined 'model' systems are of great benefit [2]. The so-called 'surface science approach' in catalysis, based on single crystal surfaces, has provided a wealth of information about the effects of defects and the crystallographic orientation on the catalytic properties of pure Pt [2,7]. Different forms of Pt-bimetallic systems explored on ideal single crystal surfaces show that the combination of the nature of the combined metal and the position of Pt atoms can be used to manipulate catalytic activity [5]. The effect of strain in the pseudomorphic monolayers, which results in a shift of the d-band centre and an alteration of the activity, is an excellent example of how the activity can be shaped by elastic deformation [4,8,9].

Pt epitaxial deposition is not readily achievable due to thermodynamic limitations that often lead to preferential 3D growth [10]. Conventional electrodeposition approaches and protocols have been explored to create high active area 3D Pt structures as a function of the ectrodeposition parameters [11–14]. Some of the methods such as 'spontaneous' deposition [15,16] and galvanic replacements of the less noble sacrificial metals [17–20] were shown as successful approaches to produce uniform 3D Pt-nanocluster networks on different substrates. All these methods provided invaluable information about the structure of high active area Pt-deposits and their catalytic behaviour.

In the last two decades, new ways to control the deposition of 2D epitaxial Pt films and sub-monolayers with atomic scale precision have been developed [21–27]. A breakthrough in epitaxial Pt monolayer growth was made by the Surface Limited Redox Replacement (SLRR) method introduced by Brankovic et al. [21]. An underpotentially deposited (UPD) epitaxial monolayer of Cu was used as a sacrificial layer to deposit a more noble Pt layer through a galvanic (redox) replacement reaction. The method has since become established as an approach to design a whole new class of highly active Pt-monolayer catalysts [4], and nonporous fuel cell functional electrodes [28–30]. Several research groups extended the SLRR methodology to grow epitaxial Pt films of different thicknesses by utilizing successive applications of the SLRR protocol in various experimental configurations such as multiple immersions and transfers of electrodes [31,32], flow-cells [22] and growth in a single-cell [23,33]. The SLRR controlled deposition of Pt films has been demonstrated with sacrificial layers other than Cu such as Pb UPD [23,34] and H UPD [33]. The advantages of using Pb UPD over Cu UPD for the growth of 2D Pt films were the quality of the epitaxial Pt layers, and the high replacement yield/efficiency that can be achieved in a single cell configuration [23]. Brankovic et al., in their detailed study of the SLRR kinetics, stressed the importance of the nature of the UPD metal as well as the solution composition on the structure and amount of deposited Pt [35,36]. It was shown that the stability of Cu (I) chloride complexes during the redox replacement in perchlorate solutions can have a profound effect on the coverage of deposited Pt resulting in half of predicted amount based on the 1:2 = Pt:Cu stoichiometric ratio [35,36].

The SLRR method has the advantage of atomic-scale control of the Pt film structure and the coverage from the sub-monolayer to several atomic layers thickness, which can be incredibly useful in the design of model-2D systems for fundamental studies in electrocatalysis [24,32,37–42]. In fact, SLRR has been used in a range of studies of electrocatalytic processes such as the oxygen reduction reaction (ORR) [4,43], the hydrogen oxidation reaction (HOR) [24], and the oxidation of small organic fuels [38,40,42] on various Pt/Au nanostructures that explored the effects of their size and thickness on reactivity. For Pt monolayers grown by Cu UPD-SLRR on different single crystal substrates, it has been argued that tensile strain in the layer influences the reactivity of Pt toward methanol and ethanol oxidation, in agreement with the theoretical predictions of the d-band model [42]. It was suggested that tensile strain of the order of 4% in pseudomorphic Pt ML/Au(111) results in the highest reactivity enhancement due to the changes of the strength of adsorption of CO and OH [42]. Bae et al. [24] studied the size effect of 2D Pt sub-monolayer clusters on the kinetics of the hydrogen oxidation reaction (HOR). It was shown that a decrease of the average tensile strain in Pt clusters on Au(111) (due to the finite size of the clusters) can have a positive effect on the kinetics of the HOR, suggesting that the activity increases with the cluster size and that a complete layer is the most active configuration of Pt for the HOR. Prieto et al. [40,41] used Cu-UPD SLRR to explore CO electrooxidation and the ethanol oxidation reaction (EOR) for sub-monolayer coverages of Pt on Au-poly and Au(hkl) stepped surfaces. Their results suggest that the Pt films were not pseudomorphic, and that significant restructuring upon CO adsorption/oxidation occurred on the Pt layers due to Pt-Au alloying which influenced the overall activity and product distribution of the EOR. Rincon et al. [32] used multiple Cu UPD-SLRR cycles to deposit Pt films and examined the effect of thickness on the electrooxidation of dissolved and adsorbed CO. They reported the formation of a complete pseudomorphic Pt ML on Au after the first redox replacement. The results showed the effect of increasing thickness of Pt films on the bond strength of CO adsorption with unusually large difference in the potentials of CO_{ad} oxidation in the presence and absence of CO in the solution. Two effects were suggested as possible explanation for the observed thickness dependence of CO electrooxidation on Pt. Firstly, the combination of the reduced strain in the Pt layers and electronic effects of the substrate with thickness could lead to a decrease in the CO adsorption toward Pt bulk values. Secondly, the increasing roughness of films could lead to a large number of low-coordination adsorption sites such as kinks and steps that also can contribute to a lowering of the CO_{ad} onset potentials with thickness.

It needs to be noted that several different groups using the same SLRR method (immersions and transfers configuration) report Pt layers of different coverages after a single replacement event [32,35,40,42]. While often the observed catalytic effects on a Pt (sub)monolayer have similar trends, their magnitudes vary. The high sensitivity of surface processes to the atomic scale structure (i.e. size and height of Pt clusters, and the roughness of the Pt overlayers) indicates that the details of SLRR protocol are very important for the observed variations in the coverages and morphology of Pt deposits. Alongside the background solutions and the metal concentration, two important aspects can contribute to the variable behaviour. One aspect is the level of oxygen in the solution and during transfer of the electrode. It has been shown that exposure to oxygen affects the stability of a UPD metal layer at the open circuit potential (OCP) [44], which might result in it becoming partially removed from the surface during the transfer or might compete with Pt ions during the redox replacement of the UPD layer. Another often neglected aspect is the time of immersion of the UPD metal covered surface in the Pt-containing solution. Once the redox replacement of a UPD layer is completed (within 10s) a spontaneous adsorption of Pt-chloride complexes takes place on the surfaces of Au and Pt [11,33]. The time scale of the spontaneous adsorption is 1–5 minutes and the application of a potential pulse to reduce this layer could add up to 0.25 ML of Pt to the deposit [11,45]. All of this suggests the significance of the SLRR kinetics and the importance of understanding the deposition steps that can affect the structure and Pt coverage on a submonolayer-to-monolayer and multilayer level.

In this work, we compare Pt ultra-thin films grown by a SLRR method in a single-cell configuration where the issues associated with the inconsistency of the conditions during growth are minimized, and the effective Pt deposition yield is maximized [23].

Pt film growth is performed using two different sacrificial UPD layers Cu and Pb that have different reduction potential, size (different UPD packing density) and replacement kinetics [24] which results in a different Pt films structure evolution with the number of replacement cycles. In agreement with the replacement kinetics and stoichiometry, we show that the electrochemically active surface area (EASA) assessed by H UPD on Pt films grown by Pb UPD produces epitaxial layers with comparable roughness, while those produced by Cu UPD show increased roughness with the number of cycles. This difference in the structure was used as a platform to explore the electrooxidation of pre-adsorbed CO_{ad} and formic acid. Specific attention has been given to the Pt films grown by a single SLRR cycle that showed most pronounced differences in the electrocatalytic behaviour and reactivity due to the Pt-Au surface configuration.

2. Experimental

2.1. Electrochemical cell and electrodes:

A standard three-electrode cell was used in Pt film deposition and electrochemical characterisation experiments. Pt wire and mercury/mercurous sulphate electrode (MSE) were used as a counter and reference electrode respectively. All potentials in this work are presented with respect to MSE. Before the electrochemical experiments, solutions were purged with ultra-pure nitrogen gas for at least 1 hour and the blanket of nitrogen gas above the solution was been maintained during measurements. All electrochemical protocols were controlled by an Ivium Compact Stat Potentiostat. All solutions were made with 18.2 MΩ Mill-Q Millipore water and the highest purity grade chemicals.

2.2. Substrates

Pt thin films were deposited on Au-polycrystalline films of 250 nm thickness produced by ultra-high-vacuum evaporation on glass slides (Schott Nexterion D) glass with 2 nm Ti adhesion layer. The evaporated Au films exhibited dominant (111) texture with average grain size of 30 nm as confirmed by X-ray diffraction θ-2θ and ex-situ STM measurements. Before each experiment the Au films were cleaned in concentrated sulphuric acid, rinsed by ultra-pure Millipore Milli-Q® water and dried in an ultra-pure nitrogen flow. A final step of the substrate preparation was flame annealing using a propane torch, which was performed by brushing the sample with a direct flame for 1 min. The annealing resulted in a defining (111) structure with an average grain size of 100–150 nm as confirmed by X-ray diffraction and ex-situ STM.

The quality of Au (111) textured films was confirmed by cyclic voltammetry measurements in 10^{-1} M H_2SO_4 (Alfa Aesar, 99.9999%) in the potential range from 0.00 V to 0.92 V with 50 mV/s. The geometric area (A) of each Au sample was determined from the charge of the Au-oxide reduction peak divided by the charge of 440 μC cm^{-2}, corresponding to a monolayer of AuO formation, $A = \frac{Q_{Au-oxide}}{440\ \mu C\ cm^{-2}}$ [46,47]. In this work the current densities of electrochemical measurements were normalised to the A of the substrate unless otherwise stated.

A Pt(111) single crystal (Metal Crystals and Oxides Ltd) of 10 mm diameter and 3.0 mm thickness was mechanically polished down to 0.05 μm alumina suspension (Buehler). Prior to experiments, the crystal was annealed for 10 minutes in a propane flame to an orange colour. The crystal was cooled in ultra-pure nitrogen atmosphere, and then transferred to an electrochemical cell for characterisation in a hanging meniscus configuration.

2.3. Pt thin film deposition

Pt thin films were deposited on Au (111) substrates by multiple SLRR cycles in a single-cell configuration using a Cu UPD or Pb UPD sacrificial layer in the presence of a $[PtCl_4]^{-2}$ complex as described in our previous work [23,37,38]. The process of growth was automated to control the application of the potential pulse of UPD layer formation (E_1), monitor the OCP changes (up to potential E_2) and repeat the desired number of SLRR cycles. The Pt films were deposited using a different number of SLRR cycles labelled by 'nR' (n = 1, 2, 5 and 10) in the text and figures.

The SLRR deposition of Pt using Pb UPD was conducted in 10^{-3} M $HClO_4$ (Aldrich, 70% redistilled), 10^{-3} M $Pb(ClO_4)_2$ (Aldrich, 99.999%), 10^{-1} M $NaClO_4$ (Aldrich, 99.999%), and 5×10^{-4} M $K_2(PtCl_4)$ (Aldrich, 99.99%) solution with potential limits of $E_1 = -0.85$ V and $E_2 = 0.00$ V [23,37]. The SLRR deposition using Cu UPD was conducted in the solution of the same background composition 10^{-3} M $HClO_4$, 10^{-1} M $NaClO_4$, 5×10^{-4} M $K_2(PtCl_4)$ just with 10^{-3} M $Cu(ClO_4)_2$ (Aldrich, 99.9999%) instead of 10^{-3} M $Pb(ClO_4)_2$. The potential limits selected in the process were $E_1 = -0.38$ V and $E_2 = 0.05$ V [23]. Following the deposition, Pt films were thoroughly rinsed with ultra-pure water and immediately transferred to the electrochemical cell for further electrochemical characterization.

2.4. Characterization of Pt thin films

The quality of Pt thin films and roughness was assessed by using cyclic voltammetry in 10^{-1} M H_2SO_4 solution at a range of potentials from −0.68 to 0.70 V with a scan rate of 50 mV/s. Following rinsing of the sample, a set of 5 CV scans was used to activate the surface [48,49]. The application of 'activation' CVs was used to ascertain removal of any passivation layer that could form during rinsing of the sample and exposure to air during the transfer between electrochemical cells. The electrochemically active surface area (EASA) of Pt films was measured using the integrated charge of hydrogen desorption (i.e. H UPD)

$$A(Pt)_{H\ upd} = \frac{Q_{H\ upd}(\mu C)}{210\ \mu C.cm^{-2}},$$

where 210 μC cm^{-2} is taken for a monolayer of H UPD on polycrystalline Pt [46,50,51].

2.4.1. CO stripping experiments

Following the H UPD characterisation, CO (research grade purity N3.7, BOC) was inserted into solution while holding the potential at −0.60 V for 5–10 min until a stable level of current was established [48,52]. Then the solution was purged with ultra-pure nitrogen for 40 min. A potential scan at 20 mV/s was applied from −0.60 V to 0.60 V to strip the adsorbed CO layer. A cyclic voltammetry scan was recorded after the stripping scan to ensure the complete CO adlayer stripping from the Pt surface, and the standard H UPD behaviour was registered.

2.4.2. Formic acid oxidation

The formic acid oxidation (FAO) measurements were done by cyclic voltammetry in 5×10^{-1} M HCOOH (Sigma-Aldrich, 98.0–100%) + 10^{-1} M H_2SO_4, between −0.68 V to 0.70 V, at a scan rate of 50 mV/s. The potential limits during FAO were the same as we used in our previous work such that all features associated with the dual pathway mechanism could be observed and that any remaining poisonous CO_{ad} could be fully oxidized and removed from the surface [38].

2.4.3. STM

Ex-situ STM characterization was done using Agilent Technologies Pico Scan 5100 system, with Pico Scan 2100 controller. The STM tips were made by etching of $Pt_{80\%}$–$Ir_{20\%}$ wire in a 1:2 mixture of saturated $CaCl_2$ solution and water at 25 V (ac).

3. Results and Discussion

3.1. SLRR deposition of Pt films

The deposition of Pt films was conducted by the SLRR method in a single cell configuration using Cu or Pb as sacrificial UPD metal layers. Following the protocol described in the previous work, Pt films of different thicknesses were deposited by successive application of SLRR cycles [23]. Briefly, each cycle consisted of a UPD layer formation by a potential pulse to a potential E_1 where complete UPD is formed initially on Au substrate and subsequently on grown Pt films. The potential pulse E_1 was applied for 1s. As described in our previous work [23], the length of the pulse allows complete UPD layer formation without any significant contribution from direct electrodeposition of Pt. This step was followed by termination of the potential control and a system was left on open circuit potential (OCP) during which spontaneous redox replacement of the UPD layer by $[PtCl_4]^{2-}$ ions takes place. During the redox replacement reaction the coverage of the UPD metal decreases, which results in an increase of the OCP until the potential E_2, corresponding to the UPD metal-free surface, is reached.

The potential limits for Pt deposition using Pb UPD-SLRR were: $E_1 = -0.85$ V and $E_2 = 0.00$ V [23]. The potential transients recorded during growth are presented alongside with the cyclic voltammograms in 10^{-1} M H_2SO_4 of Pt films deposited by a different number of SLRR cycles (labelled 'R') in Fig. 1. The OCP transients shown in Fig. 1A are very uniform and each competed in less than 10 s which is in agreement with previous work [23]. The slightly shorter length of the 1st replacement, as discussed in the previous work [23], is characteristic for SLRR growth in the single-cell configuration. The CVs of Pt films in Fig. 1B exhibit well defined peaks of H UPD in the negative potential range and the surface Pt oxidation/reduction peaks in the positive potential range. The current density of H UPD and the integrated charge (Table 1) show very small changes indicating the growth of thicker Pt films with no significant roughness increase.

The deposition of Pt films using Cu UPD-SLRR was conducted in the same perchlorate background solution to avoid any contributions other than those resulting from the different nature of a UPD metal [35,36]. The potential limits $E_1 = -0.38$ V and $E_2 = 0.05$ V were selected following the same analysis as in the case of Pb [23]. The potential transients during the replacement of Cu UPD with $[PtCl_4]^{2-}$ in Fig. 1C show a progressively longer amount of time needed to complete the red-ox replacements at OCP. The time required to complete 5 replacement cycles was almost twice as

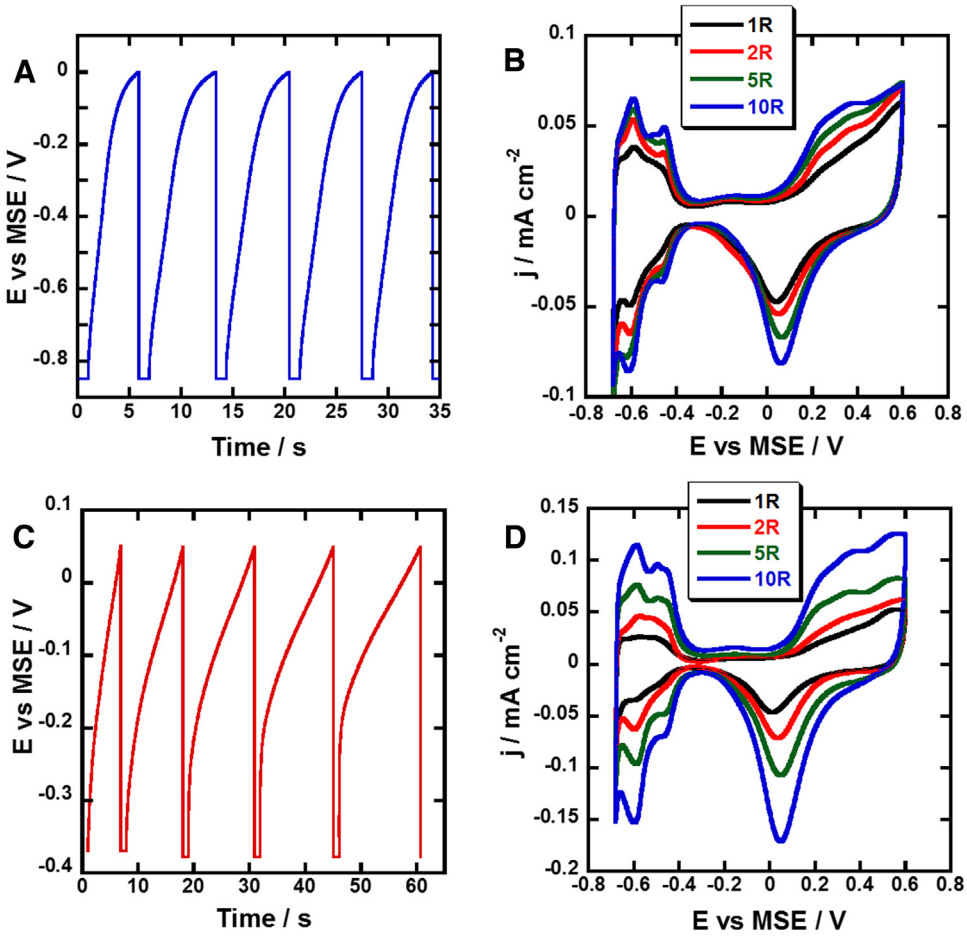

Fig. 1. Pt films grown on Au by successive SLRR cycles ('R'). (A) Potential transients during Pt deposition via SLRR of Pb UPD ($E_1 = -0.85$ V and $E_2 = 0.0$ V). (B) Cyclic voltammograms in 10^{-1} M H_2SO_4 solution ($\nu = 50$ mV/s) of Pt films grown by SLRR of Pb UPD. (C) Potential transients during Pt deposition via SLRR of Cu UPD ($E_1 = -0.38$ V and $E_2 = 0.05$ V). (D) Cyclic voltammograms in 10^{-1} M H_2SO_4 solution ($\nu = 50$ mV/s) of Pt films grown by SLRR of Cu UPD.

Table 1
Comparison of the integrated charges of H UPD ($Q_{H\ upd}$) and the roughness factor (f) of Pt films shown in Fig. 1. Films were deposited by different number of SLRR cycles (R) via SLRR of Pb and Cu.

# R	Pb UPD −SLRR		Cu UPD-SLRR	
	$Q_{H\ upd}$, μC cm^{-2}	$f = \frac{Q_{H\ upd}}{210\ \mu C\ cm^{-2}}$	$Q_{H\ upd}$, μC cm^{-2}	$f = \frac{Q_{H\ upd}}{210\ \mu C\ cm^{-2}}$
1	187 ± 19	0.90	116 ± 12	0.56
2	204 ± 20	0.97	215 ± 15	1.0
5	212 ± 20	1.01	318 ± 30	1.51
10	218 ± 20	1.04	485 ± 50	2.31

long as in the case of 5R via Pb UPD-SLRR. The first replacement step in which Pt deposits onto the Au substrate is almost two times shorter than the first cycle with Pb UPD which is in full agreement with the previously compared rates of single-step SLRR reactions of Pb UPD and Cu UPD in the perchlorate solution [36]. The increasing time of the subsequent replacement transients (R > 1) is associated with the changes of the kinetic aspects of the SLRR replacement of Cu UPD on growing Pt overlayers as shown also in the recent work by Mkwizu et al. [53]. The CV curves presented in Fig. 1D show a systematic increase of the charge associated with H UPD and more pronounced peaks associated with the (110) and (100) facets of deposited Pt. The measured EASA and estimated roughness of grown Pt films based on the H UPD charges are presented in Table 1. The Cu:Pt stoichiometry in perchlorate solutions studied by Gocken et al. [35,36]. Since the redox replacement of Cu UPD adatoms with $[PtCl_4]^{2-}$ in perchlorate solutions goes through the formation of Cu^+ complex ($[CuCl_2]^-$) due to its higher stability than Cu^{2+}, only a partial layer of Pt is deposited in each SLRR cycle [35,36]. The resultant 2:1 replacement stoichiometry can explain the increasing roughness of Pt films grown by SLRR of Cu UPD.

3.2. Pt monolayer structures on Au following a single SLRR cycle

The Pt films grown by a single SLRR cycle (1R) via Cu UPD and Pb UPD have been analysed further in more detail. The H UPD measurements confirm a higher charge density for 1R Pt films grown via Pb UPD than via Cu UPD-SLRR. Moreover, the cyclic voltammograms over an extended potential range from −0.65 to 0.92 V (~1.5 V vs RHE) in 10^{-1} M H_2SO_4 solution presented in Fig. 2 show that Pt films grown by Cu UPD-SLRR do not completely cover Au after 1R and not even after 2R. The appearance of the Au oxide reduction peak at −0.44 V is a clear indication of Au substrate exposure. The ratio of the Au oxide peak charge before and after Pt deposition suggests ~0.6 areal coverage of the surface by Pt after 1R and increases to 0.9 after 2R. It takes up to 3 SLRR cycles to completely cover the substrate. In contrast to that, a single SLRR via Pb UPD produces a Pt film that completely covers the substrate (i.e. the oxide peak is not visible).

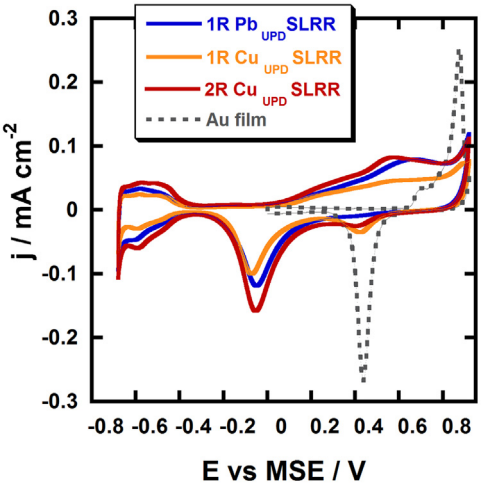

Fig. 2. Comparison of cyclic voltammograms in 10^{-1} M H_2SO_4 solution of ultra-thin Pt films grown by SLRR of Pb UPD and Cu UPD indicating the extent of Au substrate coverage. Scan rate 50 mV/s.

The difference in the morphology and coverage of the Pt layers grown by a single SLRR is illustrated by STM images in Fig. 3. The STM images are in agreement with previously reported results [23,35] and with the presented electrochemical measurements. The uniformly distributed small (~3–5 nm) Pt clusters grown by Pb UPD form a compact layer on Au while deposit grown via Cu UPD shows incomplete Au coverage and Pt clusters with a more varied size distribution. In general SLRR can proceed via two possible mechanisms: 1) 'direct exchange' where Pt and UPD metal directly exchange positions during galvanic displacement on the surface; or 2) 'local-cell' where Pt atom deposition is not necessarily the same as the UPD metals position. The uniformity of the Pt deposits independent of the surface defect distribution (such as steps and grain boundaries) is clear indication of the direct mechanism of operation during SLRR via Pb UPD. In the case of 1:2 deposition stoichiometry, two atoms of UPD metal layers are galvanically displaced with one Pt atom and the proximity of those atoms can be an issue and the contribution of the local cell mechanism is possible. An observation of more Pt deposition around the step edges in Fig. 3C might suggests a more 'local-cell' mechanism of the galvanic replacement operating during SLRR Pt deposition via Cu UPD [21,54]. However, that would contradict the proposed Cl^- ligand exchange operating during Cu redox exchange [35]. Another explanation could be an additional Pt deposited during 1 s pulse at E_1, which in single cell SLRR configuration is present albeit minimized by the length of the pulse.

The structure evolution of the deposited Pt films on Au have clear differences that will be used in following sections to explore their electrocatalytic behaviour as a function of Pt thickness and roughness. The Pb UPD grown films that completely cover Au and have comparable roughness are ideal 'model' systems for exploring strain and ligand effects on Pt catalytic behaviour. On the other hand the partial coverage of Pt on Au at lower thicknesses and the increasing roughness of Cu UPD grown films will allow us to distinguish effects of surface morphology and inhomogeneity due to the presence of high density of defects i.e. low coordination adsorption sites, as well as the exposure of the Au and Pt/Au electrode interface.

3.3. CO stripping experiments

The potentiodynamic oxidation of the adsorbed CO (CO_{ad}) on Pt films deposited by SLRR of Pb UPD and Cu UPD show clear differences of the peak shapes, and positions with thickness as presented in Fig. 4. The charges integrated under the CO stripping peaks for all films are 2 times larger (within the error) with respect to those measured by H UPD giving an estimate of the comparable surface active area: $A(Pt)_{CO} = \frac{Q_{CO}}{420\ \mu C.cm^{-2}}$, where charge of 420 μC cm^{-2} was used for a complete layer of CO_{ad} on Pt.

For Pt films grown by Pb UPD-SLRR, shown in Fig. 4(A), no significant differences of the CO stripping peak positions with film thickness can be observed. From the peak potential, E_p = 0.058 V measured for 1R (1 ML) layer the peak shifts to the E_p = 0.051 V for 10R Pt film. A small potential shift of 7 mV suggests a very small change in the strength of CO adsorption with thickness. Due to the lattice mismatch, a pseudomorphic Pt ML on Au would be under 4% tensile strain which should result in a significant positive shift of the CO stripping potential based on the d-band theory [9,55] and measurements in ultrahigh-vacuum by thermal desorption

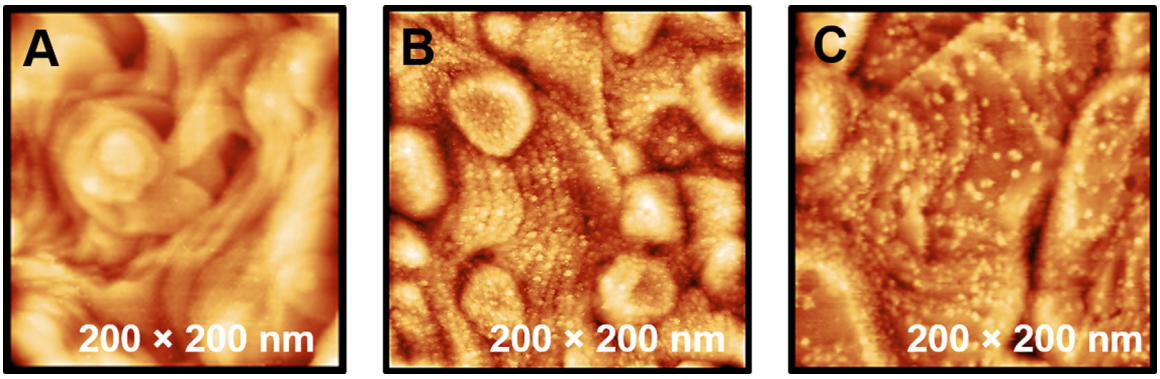

Fig. 3. Ex situ STM images of (A) bare Au substrate and Pt deposits after a single SLRR cycle via: (B) Pb UPD and (C) Cu UPD.

spectroscopy [56]. The apparent lack (or very small) of tensile strain effect on the CO electro-oxidation could be explained by the structure and morphology of Pt ML films. It is possible that Pt ML film grown by 1R is not pseudomorphic, as suggested by Prieto et al. and Brimaud et al. [27,40]. An alternative explanation could be related to the structure of the SLRR Pt deposited sub-ML films that are not smooth, as many pseudomorphic layers are, but rather consist of aligned and packed atomic height Pt nanoclusters on top of the Au substrate. Such nano-domain nature of the Pt film seems to be most stable structure as shown by Brimaud et al. [27].

In the study of Bae et al. [24] it was shown experimentally and by DFT calculations that tensile strain in sub-ML Pt nanoclusters on Au(111) is size dependent and reduces with the reduction of the average cluster size. The overall strain in the layer is then attributed to the convolution of the compressive strain (due to the finite size) and the tensile strain due to the epitaxial misfit. The study also showed that the contribution of the compressive strain in Pt-nanoclusters is most dominant and almost completely cancels out epitaxial tensile strain on clusters smaller than 8 nm diameter [24]. In our case, for 1 ML Pt grown by Pb UPD-SLRR where the average size of Pt domains is ~3–5 nm, it is possible that an almost complete balancing of the epitaxial tensile strain and size dependant compressive strain is achieved which could explain very small positive shift of the CO stripping potential, i.e. strength of adsorption, with respect to the thicker films. Furthermore, the same CO stripping peak potentials for epitaxial Pt films of higher thickness (>1ML) are in agreement with the DFT calculations by Yu et al. [57]. According to d-band model the examined CO adsorption strength on ideal epitaxial Pt films becomes smaller and almost the same as that of pure Pt when the number of layers increases above 1ML thickness [57].

On Pt films grown by Cu UPD-SLRR shown in Fig. 4B, a more pronounced difference of the stripping peak potentials with the number of SLRR cycles can be observed. For the sake of easier comparison of the onset and the peak potentials of CO stripping, the current densities of scans shown in Fig. 4B were normalized with respect the surface active area measured by CO_{ad}, i.e. $A(Pt)_{CO}$ and they are shown in the inset of Fig. 4B. The CO stripping potentials of $E_p = 0.100$ V for 1R Pt film and Ep = 0.092 V for 2R Pt films are more positive than those measured on thicker films, $E_p = 0.087$ for 5R and $E_p = 0.074$ V for 10R.The trend could be explained by epitaxial strain and finite size effects only if the average size of Pt-nanoclusters deposited via Cu UPD-SLRR is larger than those deposited by Pb UPD-SLRR. To confirm this, a detailed statistical analysis of the Pt-nanocluster size distribution conducted on Au (111) single crystal is needed which is beyond the scope of this work. A rough comparison of the STM images as well as the previous studies on this system [58] do not suggest significantly larger size of Pt-nanoclusters deposited via Cu-UPD SLRR compared to those with Pb UPD-SLRR. While strain effects cannot be excluded for medium to high coverages of Pt, other possible effects and their combination should be considered. The fact that after a single (1R) SLRR deposition with Cu UPD an incomplete Pt monolayer (0.56 ML) is formed on Au is important as

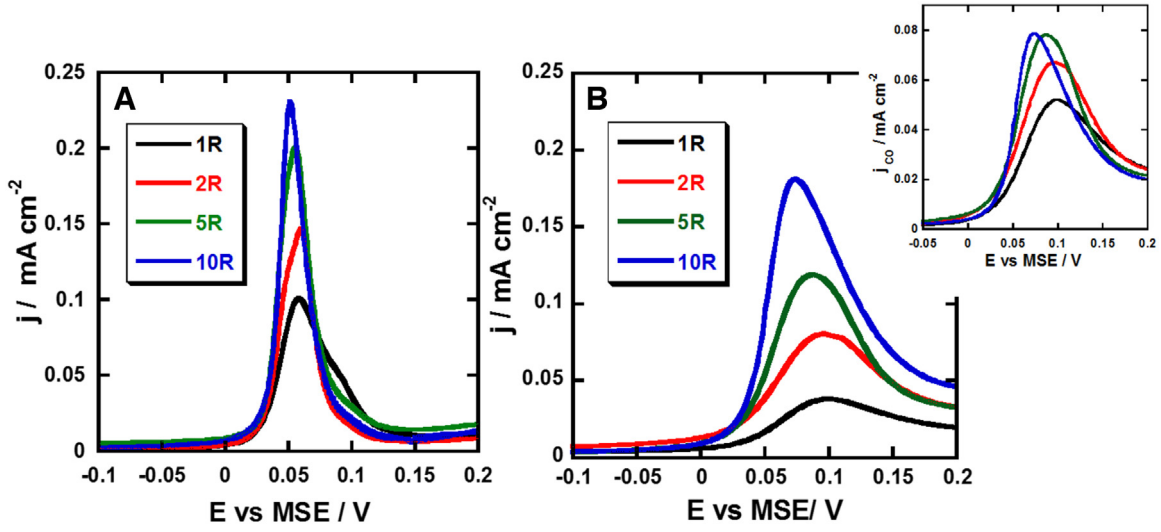

Fig. 4. CO stripping in 10^{-1} M H_2SO_4 ($\nu = 20$ mV/s) on Pt films grown by (A) SLRR of Pb UPD and (B) SLRR of Cu UPD with different number of replacement cycles. Inset (B) shows stripping curves normalized by the surface area of Pt measured by CO stripping charge.

similar positive potential shifts of the CO stripping with respect to bulk Pt have been reported on Pt-nanoclusters on Au [13–16,57,59–62] grown by different methods such as electrodeposition [13,61], spontaneous deposition [15,16,63], and SLRR [59,60]. The magnitude of the potential shift with respect to the bulk Pt vary from values larger than few hundreds of mV for very small clusters (~3 nm) [15,62] to smaller than 100 mV for larger nanoclusters (~10 nm)[13,57,59,60]. To add to the complexity, the magnitude of the potential shift also depends on the overall Pt coverage [13,60]. The most pronounced positive potential shifts have been observed for very low coverages (~0.25 ML) where most of the deposit comprises small isolated Pt-nanoclusters on Au [13,15]. Currently there is no agreement and understanding of the type of effects responsible for the positive potential shift because there are too many aspects besides strain, such as shape and coverage that could play a role which are difficult to separate. The ligand effect of Au on Pt, generally in combination with the strain effect [16,64], has been suggested as possible explanation [60]. The ensemble effect including an important role of morphology and surface defect are considered the most plausible explanations as supported by Surface Raman Spectroscopy, theoretical and DFT calculations [2,13,57,65] In that respect our results on sub-ML to ML Pt coverage further strengthen the arguments in favour of the role of structure and morphology affecting the coordination and bonding of CO on sub-ML Pt.

The results in Fig. 4B can be compared to the results of Rincon et al. [32] and Kumar et al. [60] who conducted a thickness dependence study of CO electro-oxidation on Pt films grown by Cu UPD-SLRR using a 'multiple immersion' method on polycrystalline Au in sulphate solutions. Our results are in a general agreement with these results [32] in terms of the different values of the CO stripping potentials for films grown after different number of SLRR cycles. In the work of Rincon et al. [32] there are important differences of Pt films structure contradicting the expected results and the results reported by others [60,66]. They report a completely covered Au surface after single SLRR cycle as expected based on Cu:Pt = 1:1 deposition yield in sulphate solutions. However, they show Pt films with increasing roughness with the number of SLRR cycles [32]. Although the origin of roughness evolution has neither been discussed nor quantified in their work, their results allow the comparison with the results for overlayer Pt films presented in Fig. 4A and Fig. 4B. A potential difference of ~50 mV between the peak potentials of CO stripping on 1ML and 10 ML Pt films can be estimated from Fig. 6B in their work [32]. The similar ~50 mV potential differences between the peak potentials of CO stripping on 1ML and 10 ML Pt films is measured by Kumar et al. [60]. The higher roughness of films achieved after 10 SLRR cycles in their work would certainly explain larger potential shifts toward more positive values compared to our Pt films obtained via Cu-UPD-SLRR and Pb-UPD SLRR.

Another aspect that has not been discussed so far is the UPD mediator incorporation for Pt films deposited using a single-cell SLRR. The level of sacrificial UPD metal incorporation is considered most relevant for thicker films (>1 R) where Pt deposition proceeds on a Pt surface and not on the Au substrate. The mediator incorporation can be linked to a more positive UPD stripping potential of mediators (Cu UPD and Pb UPD) on a Pt surface compared to the starting Au. The X-ray photoemission spectroscopy (XPS) measurements conducted in our previous work measured 3.5% and 3.8% of Pb incorporated into the Pt films of 10R and 40R respectively [23,37]. The work showed the CO electro-oxidation potential on 10R films (the same potential as measured in this work) is very close to the potential measured on Pt(111) (~20 mV negative) [37]. Higher levels of Pb (above 5%) incorporation result in weakening of the CO bond and more negative potential shift of the CO stripping peak. Therefore, the effect of Pb on CO stripping, at the levels incorporated in the 10R films measured here, is not significant.

In the case of Cu UPD-SLRR we do not have precise XPS measurements of the surface composition. The Energy Dispersive Spectroscopy (EDS) measurements on very thick Pt films grown by 300R cycles showed 13 at% of Cu [23]. For films grown by SLRR ofPb UPD with the same number of replacement cycles EDS showed 6 at % almost 2 times higher composition measured by XPS [23]. Therefore we can extrapolate that for 10R Cu-UPD films the upper limit of Cu composition could be in the range of 7–9%. We cannot exclude the possibility that there is an effect of Cu on the electro-oxidation which can manifest itself through ensemble and synergistic effects; for this a detailed analysis is needed which is beyond the scope of this paper. However, based on the Pt-like electrochemical behaviour of deposited films, and similarity with Pt films reported by others, we can argue that alloying might not be a dominant effect on the catalytic behaviour of these films.

3.4. Formic Acid Oxidation

FAO results on two sets of Pt films are shown in Fig. 5 where they have been normalized with respect to geometric area and EASA measured by H UPD. The FAO results normalized to geometric area (Fig. 5A and B) show clearly visible differences between two sets of samples. All Pt films grown by Pb UPD SLRR show peaks of the same height in the reversed (cathodic) scans of FAO. The behaviour is as expected for films of comparable roughness. On the FAO forward (anodic) scan two peaks can be observed. Based on the general understanding, the peak at lower potential −0.08 V is associated with the desired FAO to CO_2 (direct pathway) while the second peak between 0.24 V and 0.30 V is the peak of electro-oxidation of poisonous CO_{ad} blocking the Pt surface (indirect pathway) [67]. Fig. 5A shows that the peak at −0.08 V on forward scan is slightly higher on the 1R sample compared to the others (2–10 R) that almost match each other. The normalization with respect to H UPD (Fig. 5C) shows the same results. The behaviour of Pt films of different thicknesses during FAO can be correlated with the CO_{ad} results reported in section 3.3, suggesting that a very small change in the strength of CO adsorption on 1R films is associated with slight promotion of the direct pathway. The presence of the second peak at more positive potential ~0.25 V suggests that the indirect pathway is still operational as expected.

In a similar way, the Pt films grown with Cu UPD SLRR show more changes with the number of replacements. Fig. 5B shows increasing current peaks in the reverse and forward scans that scale with the increase of EASA for 1–10R films. Normalization of the current densities with respect to the EASA of Pt films in Fig. 5D allows us to quantify the activity enchantment by eliminating the contribution from the increased area of the samples. It is apparent from Fig. 5D, that the current increase observed as the thickness increases between 2R and 10R is mostly due to the increase in the active Pt area as the voltammograms look very similar. This is in general agreement with the behaviour observed on films grown by SLRR of Pb UPD films where the Au substrate is fully covered with Pt. However, the behaviour observed for Pt films grown after one SLRR cycle (1R) is both quantitatively and qualitatively different which suggest real increase of the reactivity in this system. The substantially higher activity in terms of the current measured during forward scan can be observed. The value of current density at the peak potentials of −0.04 V, is about ~6 times higher value than on those of higher thicknesses (5R and 10R) and about 30 times higher than the value measured on Pt (111) as shown in Fig. 6. The FAO enhanced activity on sub-ML Pt films can be correlated with the structure and size effects on CO_{ad} strength of adsorption presented in previous section. The results suggest that the activity toward FAO changes on sub-ML Pt-films by promotion

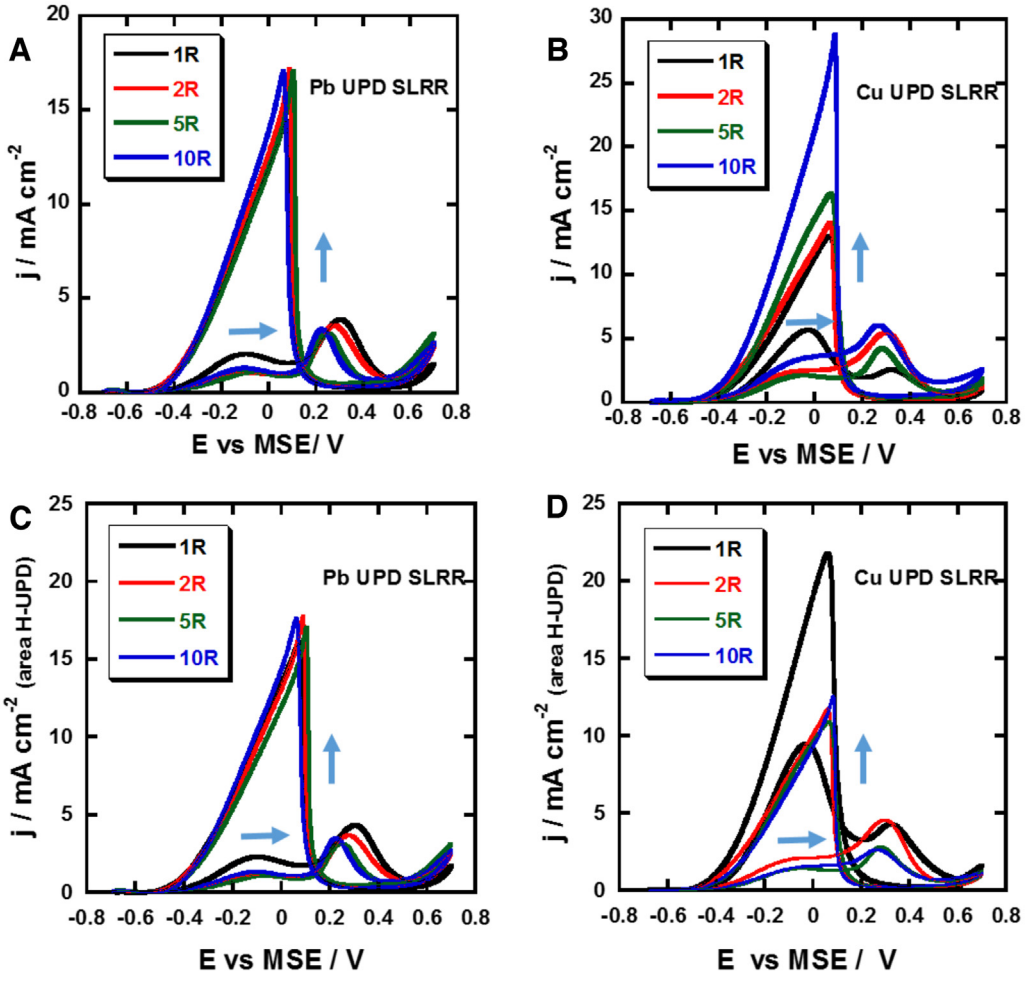

Fig. 5. Formic acid oxidation on Pt films grown by different number of SLRR cycles: (A) via Pb UPD, normalized to the geometric area of Au substrate; (B) via Cu UPD, normalized to the geometric area of Au substrate; (C) via Pb UPD, normalized to the area of Pt measured by H UPD; (D) via Cu UPD, normalized to the area of Pt measured by H UPD. Solution 5×10^{-1} M HCOOH + 10^{-1} M H_2SO_4, scan rate 50 mV/s.

of the direct pathway as shown by the increased current of the peak at lower potentials in Fig. 6. Similar FAO enhancement on Pt clusters (submonolayers) on Au has been reported on both 2D and supported nanoparticle systems [2,13–15,26,65,68,69]. The most widely accepted view of the increased activity of FAO is generally attributed to the promotion of the direct pathway due to ensemble effects [15,26,63,68] as well as the surface structure and types of defects [2,13,14,69,70]. Both reaction pathways are known to depend on the size of Pt-nanoclusters, the density and type of surface defects [70–72]. The changes in the activity of FAO reaction on sub-ML Pt cannot be related to the 'mediation' of CO poisoning, as suggested by stronger CO_{ad}, but probably to the enhanced adsorption of active reaction intermediates, presumably formate [72,73].

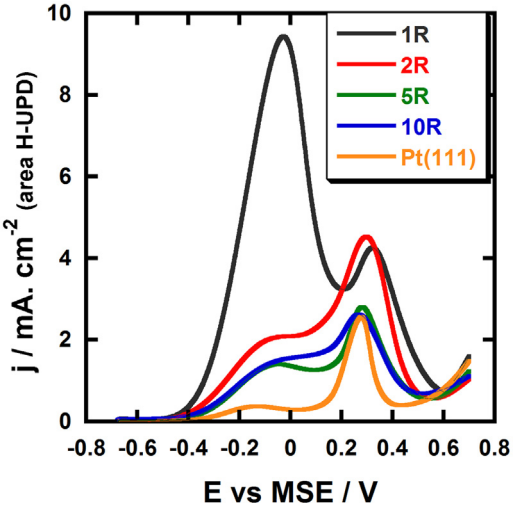

Fig. 6. Forward scans of FAO on Pt films grown by multiple SLRR cycles via Cu UPD. Solution 5×10^{-1} M HCOOH + 10^{-1} M H_2SO_4, scan rate 50 mV/s.

4. Conclusions

The structure of deposited Pt films on Au via SLRR of Pb UPD and Cu UPD have clear differences of surface morphology and structure that were used to explore the electrocatalytic behaviour of Pt films as a function of their thickness. The Pb UPD-SLRR grown films (1–10R) completely cover the Au substrate and have comparable roughness. They are an ideal 'model' 2D system to explore strain and ligand effects on CO adsorption and FAO. The results have shown no ligand effects and very small strain dependence of CO adsorption and FAO with the thickness due to the nanocluster nature of Pt films. The Pt films grown via SLRR of Cu UPD provided further insight into the effects of sub-ML Pt films on Au and the role of morphology, and coverage on the reactivity of Pt films of different roughness. The comparison with the Pb UPD grown films

suggests that the surface structure, roughness and size of the Pt-nanoclusters could be the key factors responsible for the variations of the CO_{ad} strength. The Pt films grown using a single Cu UPD-SLRR cycle were substantially more active toward FAO than other thicker films. The correlation with CO_{ad} results suggest that this enhancement is not achieved by remediation of CO poisoning but rather promotion of direct pathway related again to the structure and size of Pt-nanoclusters.

The strain effects in SLRR grown pseudomorphic Pt ML films have been widely used in the electrocatalytic community to explain the increase of a Pt monolayer's activity. Based on our results, strain effects are not very pronounced and most of the effects are probably related to the structure and roughness of the films. In summary, the observed differences in the catalytic behaviour of Pt films grown by SLRR are the result of the differences in their morphology and nanocluster structure of the films. On sub-monolayer Pt films, the behaviour is dominated by the nanocluster size and the coverage of the deposit. For a completely covered surface of Au, the effect of roughness of Pt films and nanocluster size of the deposit has a dominant role in the behaviour and activity.

Additional information

Supporting data associated with the findings reported in the paper are available at https://dx.doi.org/10.6084/m9.figshare.3413584.v1.

Acknowledgments

Z.A.A. acknowledges the support of the Oman graduate scholarship. M.P.M and N.V. acknowledge the financial support of the UK Engineering and Physical Sciences Research Council (EPSRC) as part of grant code EP/G036780/1. We thank Dr. Neil A. Fox for the deposition of Au films on glass and the Centre for Nanoscience and Quantum Information (NSQI) for providing facilities for the work. Supporting data associated with the findings reported in the paper are available at https://dx.doi.org/10.6084/m9.figshare.3413584.v1

References

[1] M.K. Debe, Electrocatalyst approaches and challenges for automotive fuel cells, Nature 486 (2012) 43–51.
[2] M.T.M. Koper, Structure sensitivity and nanoscale effects in electrocatalysis, Nanoscale 3 (2011) 2054–2073.
[3] V.R. Stamenkovic, B.S. Mun, M. Arenz, K.J. Mayrhofer, C.A. Lucas, G. Wang, P.N. Ross, N.M. Markovic, Trends in electrocatalysis on extended and nanoscale Pt-bimetallic alloy surfaces, Nat Mater 6 (2007) 241–247.
[4] R.R. Adzic, J. Zhang, K. Sasaki, M.B. Vukmirovic, M. Shao, J.X. Wang, A.U. Nilekar, M. Mavrikakis, J.A. Valerio, F. Uribe, Platinum Monolayer Fuel Cell Electrocatalysts, Top Catal 46 (2007) 249–262.
[5] F. Calle-Vallejo, M.T.M. Koper, A.S. Bandarenka, Tailoring the catalytic activity of electrodes with monolayer amounts of foreign metals, Chem. Soc. Rev. 42 (2013) 5210–5230.
[6] N.S. Porter, H. Wu, Z. Quan, J. Fang, Shape-Control and Electrocatalytic Activity-Enhancement of Pt-Based Bimetallic Nanocrystals, Accounts of Chemical Research 46 (2013) 1867–1877.
[7] N.M. Markovic, P.N. Ross, Surface science studies of model fuel cell electrocatalysts, Surface Science Reports 45 (2002) 117–229.
[8] L.A. Kibler, A.M. El-Aziz, R. Hoyer, D.M. Kolb, Tuning Reaction Rates by Lateral Strain in a Palladium Monolayer, Angewandte Chemia International Edition 44 (2005) 2080–2084.
[9] J. Greeley, J.K. Nørskov, M. Mavrikakis, Electronic structure and catalysis on metal surfaces, Annual Review of Physical Chemistry 53 (2002) 319–348.
[10] H.F. Waibel, M. Kleinert, L.A. Kibler, D.M. Kolb, Initial stages of Pt deposition on Au(111) and Au(100), Electrochim Acta 47 (2002) 1461–1467.
[11] I. Bakos, S. Szabo, T. Pajkossy, Deposition of platimun monolayers on gold, Journal of Solid State Electrochemistry 15 (2011) 2453–2459.
[12] L.M. Plyasova, I.Y. Molina, A.N. Gavrilov, S.V. Cherepanova, O.V. Cherstiouk, N.A. Rudina, E.R. Savinova, G.A. Tsirlina, Electrodeposited platinum revisited: tuning nanostructure via teh depsition potential, Electrochim Acta 51 (2006) 4477–4488.
[13] F.J.E. Scheijen, G.L. Beltramo, S. Hoeppener, T.H.M. Housmans, M.T.M. Koper, The electrooxidation of small organic molecules on platinum nanoparticles supported on gold: influence of platinum deposition procedure, J of Solid State Electrochem 12 (2008) 483–495.
[14] Obradović, Tripković, Gojković, The origin of high activity of Pt–Au surfaces in the formic acid oxidation, Electrochim Acta 55 (2009) 204–209.
[15] B. Du, Y. Tong, A coverage-dependent study of pt spontaneously deposited onto Au and Ru surfaces: direct experimental evidence of the ensemble effect for methanol electro-oxidation on Pt, J Phys Chem B 109 (2005) 17775–17780.
[16] S. Strbac, S. Petrovic, R. Vasilic, J. Kovac, A. Zalar, Z. Rakocevic, Carbon monoxide oxidation on Au(111) surface decorated by spontaneously deposited Pt, Electrochimica Acta 53 (2007) 998–1005.
[17] G. Kokkinidis, A. Papoutsis, D. Stoychev, A. Milchev, Electroless deposition of Pt on Ti—catalytic activity for the hydrogen evolution reaction, J Electroanal Chem 486 (2000) 48–55.
[18] G. Kokkinidis, D. Stoychev, V. Lazarov, A. Papoutsis, A. Milchev, Electroless deposition of Pt on Ti Part II. Catalytic activity for oxygen reduction, J Electroanal Chem 511 (2001) 20–30.
[19] S. Papadimitriou, S. Armyanov, E. Valova, A. Hubin, O. Steenhaut, E. Pavlidou, G. Kokkinidis, S. Sotiropoulos, Methanol Oxidation at Pt-Cu, Pt-Ni, and Pt-Co Electrode Coatings Prepared by a Galvanic Replacement Process, J Phys Chem C 114 (2010) 5217–5223.
[20] S. Papadimitriou, A. Tegou, E. Pavlidou, S. Armyanov, E. Valova, G. Kokkinidis, S. Sotiropoulos, Preparation and characterisation of platinum- and gold-coated copper iron, cobalt and nickel deposits on glassy carbon substrates, Electrochim Acta 53 (2008) 6559–6567.
[21] S.R. Brankovic, J.X. Wang, R.R. Adzic, Metal monolayer deposition by replacement of metal adlayers on electrode surfaces, Surface Science 474 (2001) L173–L179.
[22] Y.G. Kim, J.Y. Kim, D. Vairavapandian, J.L. Stickney, Platinum nanofilm formation by EC-ALE via redox replacement of UPD copper: Studies using in-situ scanning tunneling microscopy, J Phys Chem B 110 (2006) 17998–18006.
[23] M. Fayette, Y. Liu, D. Bertrand, J. Nutariya, N. Vasiljevic, N. Dimitrov, From Au to Pt via surface limited redox replacement of Pb UPD in one-cell configuration, Langmuir: the ACS journal of surfaces and colloids 27 (2011) 5650–5658.
[24] S.E. Bae, D. Gokcen, P. Liu, P. Mohammadi, S.R. Brankovic, Size Effects in Monolayer Catalysis—Model Study: Pt Submonolayers on Au(111), Electrocatalysis 3 (2012) 203–210.
[25] S. Ambrozik, B. Rawlings, N. Vasiljevic, N. Dimitrov, Metal deposition via electroless surface limited redox replacement, Electrochem Commun 44 (2014) 19–22.
[26] J. Kim, D. Shin, C.K. Rhee, S.-H. Yoon, Formation of Single-Layered Pt Islands on Au(111) Using Irreversible Adsorption of Pt and Selective Adsorption of CO to Pt, Langmuir: the ACS journal of surfaces and colloids 30 (2014) 4203.
[27] S. Brimaud, R.J. Behm, Electrodeposition of a Pt Monolayer Film: Using Kinetic Limitations for Atomic Layer Epitaxy, JACS 135 (2013) 11716–11719.
[28] R. Wang, C. Wang, W.-B. Cai, Y. Ding, Ultralow-Platinum-Loading High-Performance Nanoporous Electrocatalysts with Nanoengineered Surface Structures, Adv. Mater. 22 (2010) 1845–1848.
[29] H.Y. Ma, P.P. Liu, X.B. Ge, R.Y. Wang, Y. Ding, Facile Fabrication of Ultrathin Pt Overlayers onto Nanoporous Metal Membranes via Repeated Cu UPD and in Situ Redox Replacement Reaction, Langmuir: the ACS journal of surfaces and colloids 25 (2009) 561–567.
[30] D. McCurry, M. Kamundi, M. Fayette, F. Wafula, N. Dimitrov, All Electrochemical Fabrication of a Platinized Nanoporous Au Thin-Film Catalyst, ACS Appl. Mater. Interfaces 3 (2011) 4459–4468.
[31] M.F. Mrozek, Y. Xie, M.J. Weaver, Surface-enhanced Raman scattering on uniform platinum-group overlayers: preparation by redox replacement of underpotential-deposited metals on gold, Anal Chem 73 (2001) 5953–5960.
[32] A. Rincon, M.C. Perez, C. Gutierrez, Dependence of low-potential CO electrooxidation on the number of Pt monolayers on gold, Electrochim Acta 55 (2010) 3152–3156.
[33] J. Nutariya, M. Fayette, N. Dimitrov, N. Vasiljevic, Growth of Pt by surface limited redox replacement of underpotentially deposited hydrogen, Electrochim Acta 112 (2013) 813–823.
[34] N. Jayaraju, D. Viravapandian, G.Y. Kim, D. Banga, J.L. Stickney, Electrochemical Atomic Layer Deposition (E-ALD) of Pt Nanofilms Using SLRR Cycles, J Electrochem Soc 159 (2012) D616–D622.
[35] D. Gokcen, S.E. Bae, S.R. Brankovic, Stoichiometry of Pt Submonolayer Deposition via Surface-Limited Redox Replacement Reaction, J Electrochem Soc 157 (2010) D582–D587.
[36] D. Gokcen, S.E. Bae, S.R. Brankovic, Reaction kinetics of metal deposition via surface limited red-ox replacement of underpotentially deposited metal monolayers, Electrochim Acta 56 (2011) 5545–5553.
[37] M.P. Mercer, D. Plana, D.J. Fermín, D. Morgan, N. Vasiljevic, Growth of Epitaxial $Pt_{1-x}Pb_x$ Alloys by Surface Limited Redox Replacement and Study of Their Adsorption Properties, Langmuir: the ACS journal of surfaces and colloids 31 (2015) 10904–10912.
[38] M. Fayette, J. Nutariya, N. Vasiljevic, N. Dimitrov, A Study of Pt Dissolution during Formic Acid Oxidation, ACS Catalysis 3 (2013) 1709–1718.
[39] L. Bromberg, M. Fayette, B. Martens, Z.P. Luo, Y. Wang, D. Xu, J. Zhang, J. Fang, N. Dimitrov, Catalytic Performance Comparison of Shape-Dependent Nanocrystals and Oriented Ultrathin Films of Pt_4Cu Alloy in the Formic Acid Oxidation Process, Electrocatalysis 4 (2013) 24–36.

[40] M.J. Prieto, U.P.R. Filho, R. Landers, G. Tremiliosi-Filho, The ethanol electrooxidation at Pt layers deposited on polycrstalline Au, Phys. Chem. Chem. Phys. 14 (2012) 599–606.
[41] M.J. Prieto, G. Tremiliosi-Filho, Surface restructuring of Pt films on Au stepped surfaces: effects on catalytic behaviour, Phys. Chem. Chem. Phys. 15 (2013) 13184–13189.
[42] M. Li, P. Liu, R.R. Adzic, Platinum Monolayer Electrocatalysts for Anodic Oxidation of Alcohols, Journal of Physical Chemistry Letters 3 (2012) 3480–3485.
[43] M.B. Vukmirovic, J. Zhang, K. Sasaki, A.U. Nilekar, F. Uribe, M. Mavrikakis, R.R. Adzic, Platinum monolayer electrocatalysts for oxygen reduction, Electrochim Acta 52 (2007) 2257–2263.
[44] R. Vasilic, N. Vasiljevic, N. Dimitrov, Open Circuit Stability of Underpotentially Deposited Pb Monolayer on Cu(111), J. Elecatroanal. Chem. 580 (2005) 203–212.
[45] Y. Nagahara, M. Hara, S. Yoshimoto, J. Inukai, S.L. Yau, K. Itaya, In situ scanning tunneling microscopy examination of molecular adlayers of haloplatinate complexes and electrochemically produced platinum nanoparticles on Au (111), J Phys Chem B 108 (2004) 3224–3230.
[46] S. Trasatti, O.A. Petrii, Real Surface-Area Measurements in Electrochemistry, J Electroanal Chem 327 (1992) 353–376.
[47] H. Angerstein-Kozlowska, B.E. Conway, A. Hamelin, L. Stoicoviciu, Flementary steps of electrochemical oxidation of single-crystal planes of Au. Part II. A chemical and structural basis of oxidation of the (111) plane, Journal of Electroanalytical Chemistry 228 (1987) 429–453.
[48] J. Clavilier, J.M. Ortis, R. Gomez, J.M. Feliu, A. Aldaz, Comparison of electrosorption at activated polycrystalline and Pt(531) kinked platinum electrodes: surface voltammetry and charge displacement on potentiostatic CO adsorption, J. Elecatroanal. Chem. 404 (1996) 281–289.
[49] B.E. Conway, H. Angerstein-Kozlowska, W.B.A. Sharp, E.E. Criddle, Ultrapurification of Water for Electrochemical and Surface Chemical Work by Catalytic Pyrodistillation, Anal. Chem. 45 (1973) 1331–1336.
[50] D. Chen, Q. Tao, L.W. Liao, S.X. Liu, Y.X. Chen, S. Ye, Determining the Active Surface Area for Various Platinum Electrodes, Electrocatalysis 2 (2011) 207–219.
[51] Q.-S. Chen, J. Solla-Gullón, S.-G. Sun, J.M. Feliu, The potential of zero total charge of Pt nanoparticles and polycrystalline electrodes with different surface structure: The role of anion adsorption in fundamental electrocatalysis, Electrochimica Acta 55 (2010) 7982–7994.
[52] J. Clavilier, R. Albalat, R. Gomez, J.M. Ortis, J.M. Feliu, A. Aldaz, Study of the charge displacement at constant potential during CO adsorption on Pt(110) and Pt(111) electrodes in contact with a perchloric acid solution, J. Elecatroanal. Chem. 330 (1992) 489–497.
[53] T.S. Mkwizu, I. Curkowski, Physico–chemical Modelling of Adlayer Phase Formation via Surface–limited Reactions of Copper in Relation to Sequential Electrodeposition of Multilayered Platinum on Crystalline Gold, Electrochim Acta 147 (2014) 432–441.
[54] R. Vasilic, L.T. Viyannalage, N. Dimitrov, Epitaxial Growth of Ag on Au(111) by Galvanic Displacement of Pb and Tl Monolayers, J Electrochem Soc 153 (2006) C648.
[55] B. Hammer, J.K. Norskov, Theoretical surface science and catalyisis-Calculations and concepts, Advances in Catalysis 45 (2000) 71–129.
[56] M.O. Pedersen, S. Helveg, A. Ruban, I. Stensgaard, E. Laegsgaard, J.K. Norskov, F. Basenbacher, How a gold substrate can increase the reactivity of a Pt overlayer, Surface Science 426 (1999) 395–409.
[57] Y. Yu, K.H. Lim, J.Y. Wang, X. Wang, CO Adsorption Behavior on Decorated Pt@Au Nanoelectrocatalysts: A Combined Experimental and DFT Theoretical Calculation Study, The Journal of Physical Chemistry C 116 (2012) 3851–3856.
[58] D. Gokcen, Q. Yuan, S.R. Brankovic, Nucleation of Pt Monolayers Deposited via Surface Limited Redox Replacement Reaction, J Electrochem Soc 161 (2014) D3051–D3056.
[59] K.A. Friedrich, F. Henglein, U. Stimming, W. Unkauf, Size dependence of the CO monolayer oxidation on nanosized Pt particles supported on gold, Electrochim Acta 45 (2000) 3283–3293.
[60] S. Kumar, S. Zou, Electrooxidation of carbon monoxide and methanol on platinum-overlayer-coated gold nanoparticles: effects of film thickness, Langmuir: the ACS journal of surfaces and colloids 23 (2007) 7365–7371.
[61] M.N. Desic, M.M. Popovic, M.D. Obradovic, L.M. Vracar, B.N. Grgur, Study of gold-platinum and platinum-gold surface modification and its influence on hydrogen evolution and oxygen reduction, Journal of Serbian Chemical Society 70 (2005) 231–241.
[62] F. Maillard, M. Eikerling, O.V. Cherstiouk, S. Schreier, E. Savinova, U. Stimming, Size effects on reactivity of Pt nanoparticles in CO monolayer oxidation: The role of surface mobility, Faraday Discussions 125 (2004) 357.
[63] J. Kim, J. Lee, S. Kim, Y.-R. Kim, C.K. Rhee, Contrasting Electrochemical Behavior of CO, Hydrogen, and Ethanol on Single-Layered and Multiple-Layered Pt Islands on Au Surfaces, J Phys Chem C 118 (2014) 24425–24436.
[64] J.R. Kitchin, J.K. Norskov, M.A. Barteau, J.G. Chen, Role of strain and ligand effects in the modification of the electronic and chemical properties of bimetallic surfaces, Phys Rev Lett 93 (2004) 156801.
[65] Y. Yu, Y. Hu, X. Liu, W. Deng, X. Wang, The study of Pt@Au electrocatalyst based on Cu underpotential deposition and Pt redox replacement, Electrochimica Acta 54 (2009) 3092–3097.
[66] R. Loukrakpam, Q. Yuan, V. Petkov, L. Gan, S. Rudi, R. Yang, Y. Huang, S.R. Brankovic, P. Strasser, Efficient C-C bond splitting on Pt monolayer and sub-monolayer catalysts during ethanol electro-oxidation: Pt layer strain and morphology effects, Phys Chem Chem Phys 16 (2014) 18866–18876.
[67] A. Capon, R. Parsons, The oxidation of formic acid on noble metal electrodes: II. A comparison of the behaviour of pure electrodes, Journal of Electroanalytical Chemistry and Interfacial Electrochemistry 44 (1973) 239–254.
[68] S.H. Ahn, Y. Liu, T.P. Moffat, Ultrathin Platinum Films for Methanol and Formic Acid Oxidation: Activity as a Function of Film Thickness and Coverage, ACS Catalysis 5 (2015) 2124–2136.
[69] F. Maillard, S. Pronkin, E.R. Savinova, Size effects in electrocatalysis of fuel cell reactions on supported metal nanoparticles, in: M.T.M. Koper (Ed.), Fuel Cell Catalysis a Surface Science Approach, John Wiley&Sons Inc., Hoboken, NY, 2009, pp. 507–566.
[70] V. Grozovski, J. Solla-Gullo'n, V.c. Climent, E. Herrero, J.M. Feliu, Formic Acid Oxidation on Shape-Controlled Pt Nanoparticles Studied by Pulsed Voltammetry, Journal of Physical Chemistry C 114 (2010) 13802–13812.
[71] V. Grozovski, V. Climent, E. Herrero, J.M. Feliu, Intrinsic activity and poisoning rate for HCOOH oxidation at Pt(100) and vicinal surfaces containing monoatomic (111) steps, Chemphyschem 10 (2009) 1922–1926.
[72] V. Grozovski, F.J. Vidal-Iglesias, E. Herrero, J.M. Feliu, Adsorption of formate and its role as intermediate in formic acid oxidation on platinum electrodes, Chemphyschem 12 (2011) 1641–1644.
[73] Y.X. Chen, A. Miki, S. Ye, H. Sakai, M. Osawa, Formate, an Active Intermediate for Direct Oxidation of Methanol on Pt Electrode, J Am Chem Soc 125 (2003) 3680–3681.